Journal of Pharmaceutical Sciences

NOVEMBER 1977
VOLUME 66 NUMBER 11

RESEARCH ARTICLES

Degradation Kinetics of a Novel Antimitogenic and Antiviral Palladium(II) Coordination Compound

ANWAR B. BIKHAZI *x, SARKIS M. AGHAZARIAN *, and HASSAN A. TAYIM ‡

Abstract □ The degradation kinetics of a new organometallic coordination compound, aquadichloro(2,6-diaminopyridine)palladium(II), were studied in acidic and acid halide media. In acidic solutions, the degradation was first order with respect to the complex concentration; *e.g.*, at 77°, the apparent rate constants at pH 1.00, 1.22, and 1.50 were 0.00395, 0.00292, and 0.00225 min^{-1}, respectively. Furthermore, a plot of log (apparent rate constant) *versus* pH gave a straight line with an approximate slope of 0.5, indicating pseudo-first-order catalysis with respect to complex concentration at a specified pH. Activation energies obtained from Arrhenius plots varied from 43 to 57 kcal/deg/mole for pH 1.00 and 1.50, respectively. The pH-independent activation energy was 15 kcal/deg/mole. In acid halide solutions, utilizing the method of initial rates, the degradation was first order with respect to complex concentration. A plot of log (initial rate) *versus* log (chloride-ion concentration) gave a straight line with an apparent slope of 1.0. A plot of log (initial rate) *versus* pH resulted in a straight line with a slope of 0.5. Thus, pseudo-first-order catalysis with respect to complex concentration at a specified pH and pCl occurred. When the method of curve stripping was applied to the data, a plot of log (complex concentration undegraded) *versus* time resulted in a biexponential relationship; *e.g.*, at pH 1.50, 0.10 *M* chloride concentration, and 57°, the biexponential relationship between undegraded complex *versus* time giving the best fit to the data was: complex concentration = $0.237e^{-0.0653t} + 2.213e^{-0.00276t}$. A general mechanistic explanation of the acid- and acid halide-catalyzed degradation of the complex is proposed.

Keyphrases □ Palladium(II) coordination compound—degradation kinetics in acidic and acid halide media □ Aquadichloro(2,6-diaminopyridine)palladium(II)—degradation kinetics in acidic and acid halide media □ Coordination compounds—aquadichloro(2,6-diaminopyridine)palladium(II), degradation kinetics in acidic and acid halide media □ Degradation kinetics—aquadichloro(2,6-diaminopyridine)palladium(II) in acidic and acid halide media □ Stability—aquadichloro(2,6-diaminopyridine)palladium(II) in acidic and acid halide media

The therapeutic significance of organometallic coordination compounds as antiviral, antimitogenic, and antitumor agents gained importance recently (1, 2). Different theories have been proposed for their mode of action (3–5), but none is fully validated. Previous studies on the mechanism of degradation of organometallic coordination compounds were concerned with thermal stability, acid and base catalysis, anation, and other substitution reactions (6–21).

The present paper reports a study of the stability of aquadichloro(2,6-diaminopyridine)palladium(II)[1] in acidic and acid halide media and calculation of rate constants, pseudo-order constants, activation energies, and equilibrium constants. Furthermore, general mechanistic explanations of the catalytic reactions are proposed.

EXPERIMENTAL

Synthesis of Aquadichloro(2,6 - diaminopyridine)palladium(II)—The procedure followed was reported recently (20).

Standard Curves—Appropriate dilutions of the coordination compound and its ligand 2,6-diaminopyridine were prepared in acidic, neutral, and basic media. The UV spectra were recorded on a UV spectrophotometer[2], and the λ_{max} was determined. Standard solutions of the complex and the ligand were then prepared in their corresponding media and assayed spectrophotometrically using appropriate blanks. The molar absorptivities (ϵ^{M}_{1cm}) calculated from the standard curves are reported in Table I.

Analytical Procedures—Solutions of both the ligand and the complex were prepared in various aqueous media at different pH values. Spectral interference between the ligand and the complex were noted for possible use as an analytical assay procedure for the complex and/or the ligand in the presence of one another. At λ_{max} 340 nm, the complex and the ligand did not interfere in basic media (Table I). Therefore, for

[1] Previously referred to in the literature as palladium dichloride (2,6-diaminopyridine)·H_2O.
[2] Model 202, Perkin-Elmer Corp., Norwalk, Conn.

Table I—Estimated λ_{max} Values and Molar Absorptivities ($\epsilon^{M}_{1\,cm}$) of the Ligand and the Complex in Acidic and Basic Media

Compound	Medium	λ_{max}, nm	$\epsilon^{M}_{1\,cm}$
Ligand	Acid, pH 1–2	332	13,550
		243	9,000
	Base, pH 11	240	7,600
		304	7,325
		340	0
Complex	Acid, pH 1–2	Unstable	—
	Base, pH 11	340	4,270
		304[a]	3,590

[a] At $\lambda_{304\,nm}$, complex showed no maximum; $\epsilon_1{}^{M}_{cm}$ at 304 was calculated from absorbance.

stability studies in acidic media, the samples were made basic and read at λ_{max} 340 nm for the undegraded complex. Thus, the following relationship is proposed:

$$\frac{A_{340\,nm}}{\epsilon^{M}_{1\,cm\,(340\,nm)}} = \frac{A_{304\,nm}}{\epsilon^{M}_{1\,cm\,(304\,nm)}} \qquad \text{(Eq. 1)}$$

where A is the absorbance, and $\epsilon^{M}_{1\,cm}$ is the molar absorptivity as reported in Table I. Therefore, it is possible to calculate the absorbance of the complex at 304 nm once $\epsilon^{M}_{1\,cm\,(340\,nm)}$ and $\epsilon^{M}_{1\,cm\,(304\,nm)}$ are known; the value of $A_{340\,nm}$ of the complex is experimentally determined in basic media. This procedure allowed for the analysis of both the ligand and the complex in the presence of one another in any reaction mixture.

Acid Catalysis Procedure—A saturated solution of the complex (7.35×10^{-4} *M*) was prepared in double-distilled water and then diluted in the corresponding acidic medium (30 ml total volume in the reaction flask), with absorbance values ranging between 0.1 and 1.0 at the specific λ_{max}. The reaction flask was preequilibrated at the desired temperature (37–77°) in a thermostatically controlled water bath.

After thermal equilibration was completed, the desired quantity of acid was added to the mixture for the initiation of the reaction. The zero time was immediately recorded, and a 2-ml sample was withdrawn from the reaction flask. The sample was transferred into a precooled test tube in crushed ice for reaction quenching. Samples were similarly withdrawn at different time intervals. At the end of the experiment, 2.0–6.0 ml of 0.1 *N* sodium hydroxide solution was added to the 2.0-ml samples to make the final pH basic. The samples were then spectrophotometrically assayed as discussed under *Analytical Procedures*.

Equilibrium Studies—Acid catalytic reactions were allowed to reach equilibrium as spectrophotometrically observed. The following mathematical relationships were deduced from the reaction mechanism proposed under *Discussion:*

$$K_{eq} = \frac{[Pd(H_2O)_4][LH_2{}^{2+}]}{[Pd(X_2)L]} \qquad \text{(Eq. 2)}$$

where $Pd(X_2)L$ represents the complex, X is chloride, and L is 2,6-diaminopyridine. When $[Pd(H_2O)_4] = [LH_2{}^{2+}]$, then:

$$K_{eq} = \frac{[LH_2{}^{2+}]^2}{[Pd(X_2)L]} \qquad \text{(Eq. 3)}$$

Acid Halide Catalysis Procedure—The halides included chloride and bromide ions. Experiments with iodides and fluorides were not possible because iodides liberated iodine and fluorides liberated hydrogen fluoride gas in acidic media. The procedure for acid halide catalysis was basically the same as that described under *Acid Catalysis Procedure*. However, to assess the effect of the halide ion, perchloric acid was used to acidify the solution; the perchlorate ion has no catalytic effect on the reaction.

Therefore, to the preequilibrated stock solution of the complex in the water bath, a pipetted quantity of a concentrated solution of halide ions was added. The final halide-ion concentration in the reaction mixture varied from 3.3×10^{-3} to 10^{-1} *M*, depending on the experiment. Then, the required amount of concentrated perchloric acid was added, and sampling was exactly the same as described under *Acid Catalysis Procedure*. Both the chloride and bromide ions showed identical effects on the reaction process, so sodium chloride was used as the halide source.

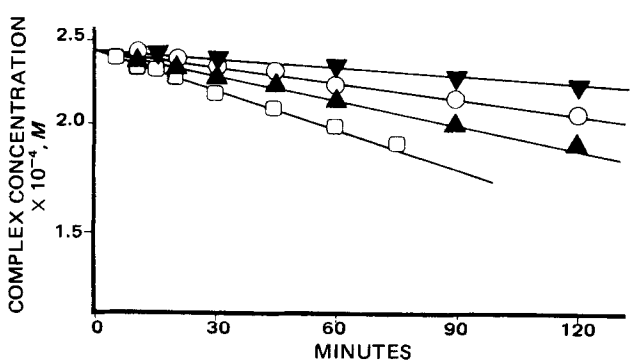

Figure 1—*Semilogarithmic plot of complex concentration undegraded* $\times 10^{-4}$ M versus *time in minutes in acid catalysis experiment at pH 1.0 (thermal stability study). Key:* ▼, *57°;* ○, *67°;* ▲, *72°; and* □, *77°.*

Table II—Calculated Rate Constants in Acid Catalysis of Complex while Varying pH and Temperature and Keeping Complex Concentration Constant

Temperature	pH[a]	Rate Constant, $k_{obs}{}^{b} \times 10^{-3}$, min^{-1}	Rate Constant, $k_H{}^{c} \times 10^{-3}$, liters/mole/min
77°	1.00	3.95	
77°	1.22	2.92	12.7
77°	1.50	2.25	
72°	1.00	2.35	
72°	1.22	1.97	8.0
72°	1.50	1.35	
67°	1.00	1.67	
67°	1.22	1.10	6.25
67°	1.50	0.83	

[a] The pH measurement at the end of the experiment at 25°. [b] Calculated from slope of lines on semilogarithmic plots, and $k_{obs} = k_H[H^+]^{0.5}$. [c] Calculated from slope of lines on rectangular plots when k_{obs} *versus* $[H^+]^{0.5}$ is drawn.

Calculations and Data Treatment—The theory proposed for acid catalysis is based on the following reaction mechanism of the complex:

$$Pd(X_2)L + 4H_2O + 2H^+ \rightleftharpoons Pd(H_2O)_4{}^{2+} + 2X^- + LH_2{}^{2+}$$

Scheme I

The general rate equation for the acid catalytic process is written as:

$$\frac{d[Pd(X_2)L]}{dt} = k_{(H)}[H_2O]^p[H^+]^m[Pd(X_2)L]^n \qquad \text{(Eq. 4)}$$

where $k_{(H)}$ represents the true rate constant for hydrogen-ion catalysis, brackets denote concentration, and the superscripts p, m, and n refer to the order of the reaction with respect to water, hydrogen-ion, and complex concentrations, respectively. It is generally assumed that $[H_2O]$ and $[H^+]$ are constant in the reaction mixture. Thus, Eq. 4 is reduced to the following general pseudo-order rate equation:

$$\frac{d[Pd(X_2)L]}{dt} = k_{obs}[Pd(X_2)L]^n \qquad \text{(Eq. 5)}$$

where:

$$k_{obs} = k_H[H_2O]^p[H^+]^m \qquad \text{(Eq. 6)}$$

Equation 6 can be written as:

$$\log k_{obs} = \log k_H[H_2O]^p - m\text{pH} \qquad \text{(Eq. 7)}$$

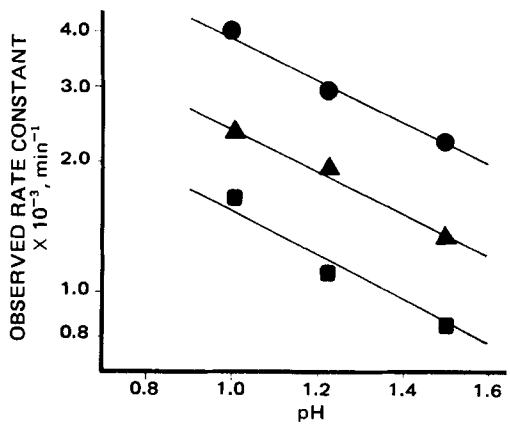

Figure 2—*Semilogarithmic plot of* $k_{obs} \times 10^{-3}$ *in minutes*$^{-1}$ versus *pH in acid catalysis experiment at different temperatures. Key:* ■, *67°;* ▲, *72°; and* ●, *77°.*

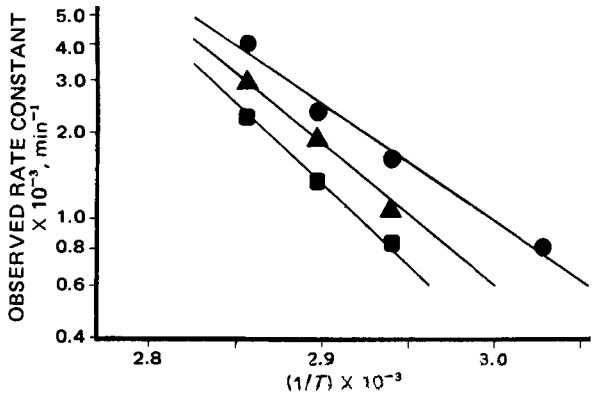

Figure 3—*Arrhenius plot for acid catalysis experiments at different pH values. Key:* ■, *pH 1.50;* ▲, *pH 1.22; and* ●, *pH 1.0.*

The following Arrhenius relationship is used in the thermal stability studies in acidic media of the complex:

$$\log k_{obs} = \log A - \frac{\Delta H}{2.3RT} \qquad \text{(Eq. 8)}$$

where A is the Arrhenius constant, R is the gas constant, ΔH is the activation energy of the reaction, and T is the temperature in absolute degrees.

The reaction mechanism proposed for acid halide catalysis is:

$$Pd(X_2)L + H_2O + 2X^- + 2H^+ \rightarrow Pd(X_4)^{2-} + LH_2^{2+}$$

Scheme II

Therefore, the general rate equation for acid halide catalysis is written as:

$$\frac{d[Pd(X_2)L]}{dt} = k_{(H)(Cl)}[H^+]^{p'}[Cl^-]^{m'}[Pd(X_2)L]^{n'} \qquad \text{(Eq. 9)}$$

where $k_{(H)(Cl)}$ represents the true rate constant for hydrogen-ion–chloride catalysis. The method of initial rate is proposed in the treatment of the data. This method is used by keeping two out of the three variable species in the reaction mixture constant. Then, a plot of log (initial rate of complex degrading) *versus* log (species concentration) results in a straight line with a slope p', m', or n', depending on which species in the reaction is the variable.

Since the data on acid halide catalysis did not fit a zero-, first-, second-, or higher order process, such a complicated mechanism possibly fits a biexponential relationship. This relationship was found to agree with the results when log $[Pd(X_2)L]$ *versus* time was plotted semilogarithmically according to Eq. 10:

$$[Pd(X_2)L] = Ae^{-\alpha t} + Be^{-\beta t} \qquad \text{(Eq. 10)}$$

where A and B represent concentration terms, which at time (t) zero would add up to the initial complex concentration; and α and β stand for the complicated rate constants of the reaction and are possibly functions of chloride- and hydrogen-ion concentrations. The method of curve stripping allows the calculations of both α and β.

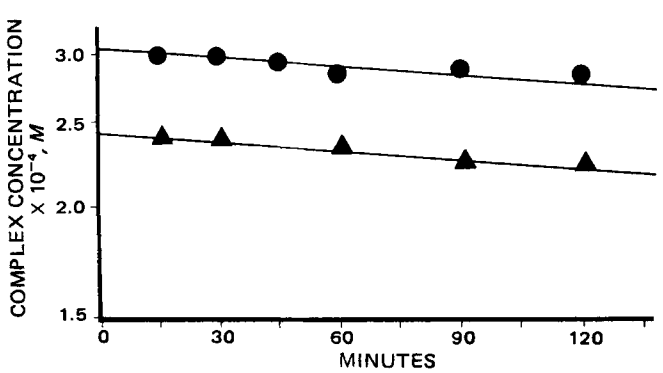

Figure 4—*Semilogarithmic plot of complex concentration undegraded* $\times 10^{-4}$ M versus *time in minutes in acid catalysis experiment at pH 1.0 and 57° while varying the initial complex concentration. Key:* ▲, *2.45* $\times 10^{-4}$ M; *and* ●, *3.06* $\times 10^{-4}$ M.

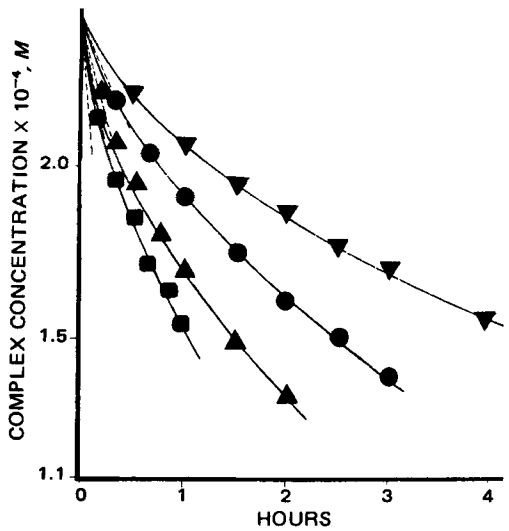

Figure 5—*Plot of complex concentration* $\times 10^{-4}$ M versus *time in hours in acid halide catalysis experiment at chloride-ion concentration of* 10^{-1} M *and 57° while varying the pH. Key:* ▼, *pH 2.20;* ●, *pH 1.50;* ▲, *pH 1.30; and* ■, *pH 1.1.*

RESULTS

Acid Catalysis—The three variables influencing the acid catalytic mechanism of the complex are the complex concentration, pH, and temperature. Therefore, this catalytic mechanism was studied as a function of each variable. For example, Fig. 1 represents a plot of the logarithm of complex concentration remaining in the reaction mixture *versus* time in a system where the initial complex concentration and the pH were constant, the only variable being the temperature. Linearity is observed in the plots for all systems when complex concentration *versus* time is plotted semilogarithmically (Table II).

Figure 2 is a graphical illustration of Eq. 7 for a plot of log k_{obs} *versus* pH of the data as reported in Table II. The average slope of the lines was 0.5 and equal to m in Eq. 7.

Figure 3 is the Arrhenius plot of log k_{obs} *versus* reciprocal temperature (in absolute degrees) of the data presented in Table II. The activation energies calculated from the slopes of the lines were 43 kcal/deg/mole at pH 1.00, 50 kcal/deg/mole at pH 1.22, and 57 kcal/deg/mole at pH 1.50. The variation in the activation energies is explained on the basis that the rate constants are pH dependent. Also, when the data of k_H reported in Table II were plotted as log k_H *versus* reciprocal temperature, a straight line resulted. The slope of this linear plot made it possible to calculate

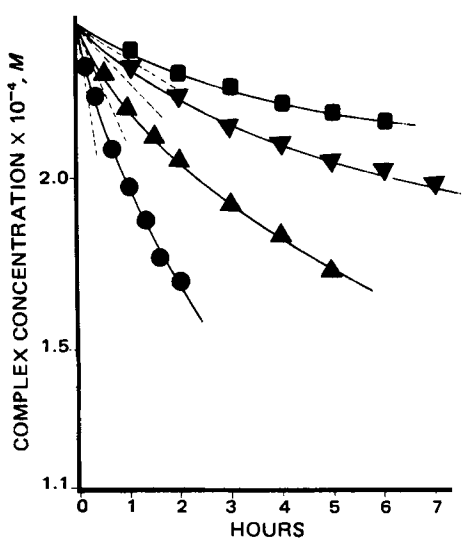

Figure 6—*Plot of complex concentration* $\times 10^{-4}$ M versus *time in hours in acid halide catalysis experiment at pH 1.1 and 47° while varying the chloride-ion concentration. Key:* ■, *3.3* $\times 10^{-3}$ M; ▼, *1* $\times 10^{-2}$ M; ▲, *3.3* $\times 10^{-2}$ M; *and* ●, *1* $\times 10^{-1}$ M.

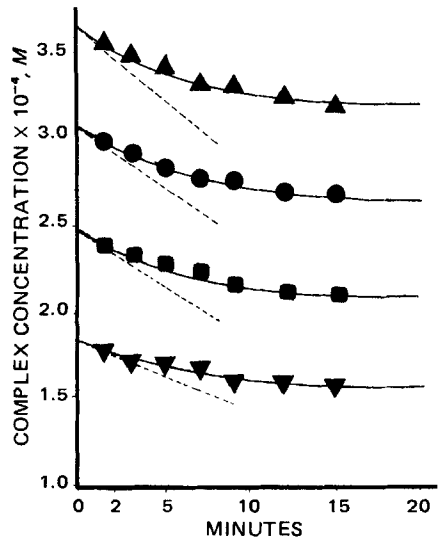

Figure 7—*Plot of complex concentration* × 10^{-4} M versus *time in minutes in acid halide catalysis experiment at pH 1.1, 57°, and a chloride-ion concentration of* 10^{-1} M *while varying the initial complex concentration. Key:* ▼, *1.84* × 10^{-4} M; ■, *2.45* × 10^{-4} M; ●, *3.07* × 10^{-4} M; *and* ▲, *3.7* × 10^{-4} M.

an activation energy of around 15 kcal/deg/mole, which is pH independent.

Figure 4 shows the effect of varying the complex concentration on the reaction mechanism. The semilogarithmic plots are linear and parallel. Thus, the data reported so far supported the fact that the reaction mechanism is hydrogen-ion catalyzed and pseudo-first order with respect to complex concentration. Therefore, Eq. 4 can be written as:

$$\frac{d[Pd(X_2)L]}{dt} = k_{(H)}[H^+]^{0.5}[Pd(X_2)L]^1 \qquad \text{(Eq. 11)}$$

Equilibrium Studies—The calculated K_{eq} values utilizing Eq. 3 were 1.475×10^{-4} at pH 1.10, 0.574×10^{-4} at pH 1.50, and 0.325×10^{-4} at pH 1.70. Thus, the K_{eq} values are dependent on hydrogen-ion concentration. Therefore, a normalized K_{eq} value was calculated by dividing the calculated K_{eq} value by the hydrogen-ion concentration. These normalized values are 1.69×10^{-3} at pH 1.1, 1.77×10^{-3} at pH 1.50, and 1.70×10^{-3} at pH 1.70. The normalized values are almost equal and are independent of the hydrogen-ion concentration.

Acid Halide Catalysis—The results of the acid halide catalysis depended on the following: (*a*) the effect of varying the hydrogen-ion concentration on the degradation mechanism of the complex while keeping the initial complex concentration, chloride-ion concentration, and temperature constant; (*b*) the effect of varying the chloride-ion concentration while keeping the concentration of the other variables constant; and (*c*) the effect of varying the complex concentration while keeping the concentrations of the other two variables constant.

Table III—Estimated Initial Rates of Degradation of Complex in Acid Halide Media while Keeping Temperature, pH, and Complex Concentration Constant

pH	Temperature	Chloride-Ion Concentration, *M*	Initial Rate × 10^{-7}, *M*/min
1.10	47°	0.10	16.2
	47°	0.033	6.57
	47°	0.010	2.43
	57°	0.10	60.0
	57°	0.033	23.2
	57°	0.010	9.08
1.50	57°	0.10	32.5
	57°	0.033	11.5
	57°	0.010	5.18
	67°	0.10	85.0
	67°	0.033	34.3
	67°	0.010	14.0

Table IV—Estimated Initial Rates of Degradation of Complex in Acid Halide Media while Keeping Temperature (57°), Chloride Concentration, and Complex Concentration Constant

pH	Initial Rate × 10^{-7}, *M*/min
1.1	60.00
1.3	43.00
1.5	32.50
2.2	13.40

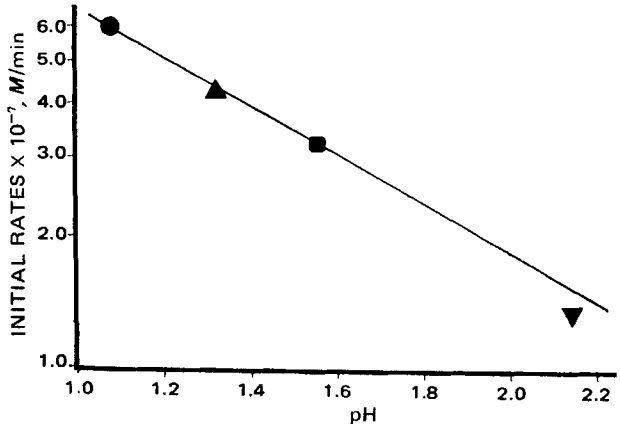

Figure 8—*Semilogarithmic plot of estimated initial rates* × 10^{-7} *in* M/*min* versus *pH in acid halide catalysis experiment at 57° and a chloride-ion concentration of* 10^{-1} M. *Key:* ▼, *pH 2.20;* ■, *pH 1.50;* ▲, *pH 1.30; and* ●, *pH 1.10.*

Figures 5–7 represent these studies when complex concentration is plotted *versus* time on rectangular coordinates. The initial slopes of the plots are calculated and presented in Tables III and IV. Figure 8 represents a plot of log initial rate *versus* pH of the data in Tables III and IV. The slope of the line was 0.5 and equal to p' in Eq. 9. Figure 9 shows the log–log plot of initial rate *versus* chloride concentration at different temperatures as given in Table III. The averaged slope of the lines was around 1.0 and equal to m' in Eq. 9. Similarly, Fig. 10 is a log–log plot of initial rate *versus* complex concentration. The slope of the line was 1.0 and equal to n' in Eq. 9. Therefore, Eq. 9 can be written as:

$$\frac{d[Pd(X_2)L]}{dt} = k_{(H)(Cl)}[H^+]^{0.5}[Cl^-]^1[Pd(X_2)L]^1 \qquad \text{(Eq. 12)}$$

Curve-Stripping Procedure and Residuals—Figure 11 is a semilogarithmic plot of three sets of data for acid halide catalysis. The biexponential shape of the curves is mathematically supported by Eq. 10; therefore, at t large and when $\alpha \gg \beta$, the slope is estimated to be β. The value of α is then obtained by extrapolation of the linear portion of the plot fitting $Be^{-\beta t}$. Therefore, subtracting the subsequent values, at t small, of the extrapolated line from the values of the curved portion of the plot would give residual values. Thus, Eq. 10 is rearranged to give:

$$\text{residual} = [Pd(X_2)L] - Be^{-\beta t} = Ae^{-\alpha t} \qquad \text{(Eq. 13)}$$

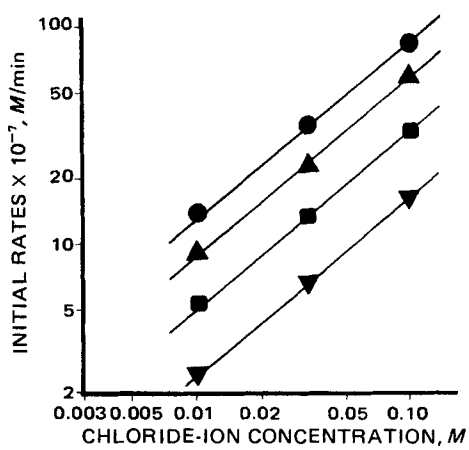

Figure 9—*Log–log plot of estimated initial rates* × 10^{-7} *in* M/*min* versus *chloride-ion concentration in* M *in acid halide catalysis experiment while varying pH and temperature. Key:* ●, *pH 1.1, 47°;* ▲, *pH 1.5, 57°;* ■, *pH 1.1, 57°; and* ▼, *pH 1.5, 67°.*

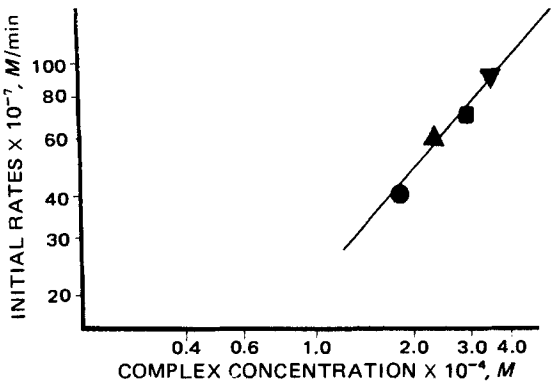

Figure 10—*Log-log plot of estimated initial rates* $\times 10^{-7}$ *in* M/*min* versus *complex concentration* $\times 10^{-4}$ M *in acid halide catalysis experiment at pH 1.1, 57°, and a chloride-ion concentration of* 10^{-1} M *while varying initial complex concentration. Key:* ●, 1.84×10^{-4} M; ▲, 2.45×10^{-4} M; ■, 3.07×10^{-4} M; *and* ▼, 3.7×10^{-4} M.

A semilogarithmic plot of residuals *versus* time, *t*, gave straight lines with slopes equal to α (Fig. 11). Table V gives the values of α, β, *A*, and *B* for the experiments on acid halide catalysis as calculated by the curve-stripping method.

DISCUSSION

The present study explained the mechanism of degradation of aquadichloro(2,6-diaminopyridine)palladium(II) in acidic and acid halide media. For acid catalysis, an overall order of 1.5 with respect to the reacting species in the reaction mixture was observed. The calculated activation energies revealed an extremely sensitive process with acid catalysis. The general reaction mechanism for acid catalysis can be proposed as occurring in two steps, a possible aquation reaction (Scheme III) and acid catalysis (Scheme IV).

The acid halide catalysis process had an overall order of 2.5 with respect to the reacting species. It was also demonstrated by the curve-stripping method that a biexponential relationship easily fit the results. For example, from Table V, when the pH is 1.50, *T* is 57°, chloride concentration is 10^{-1} *M*, and $[Pd(X_2)L]_{t=0}$ is 2.45×10^{-4} *M*, the following relationship

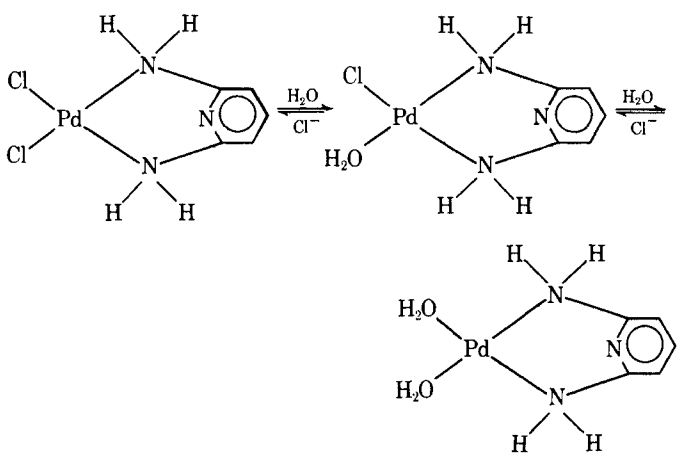

Scheme III

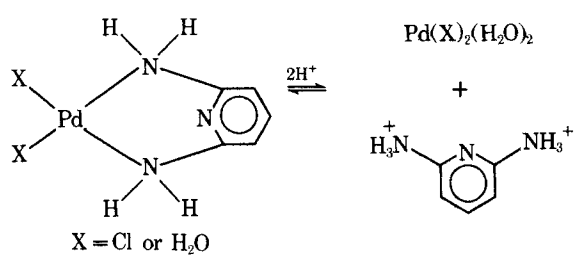

Scheme IV

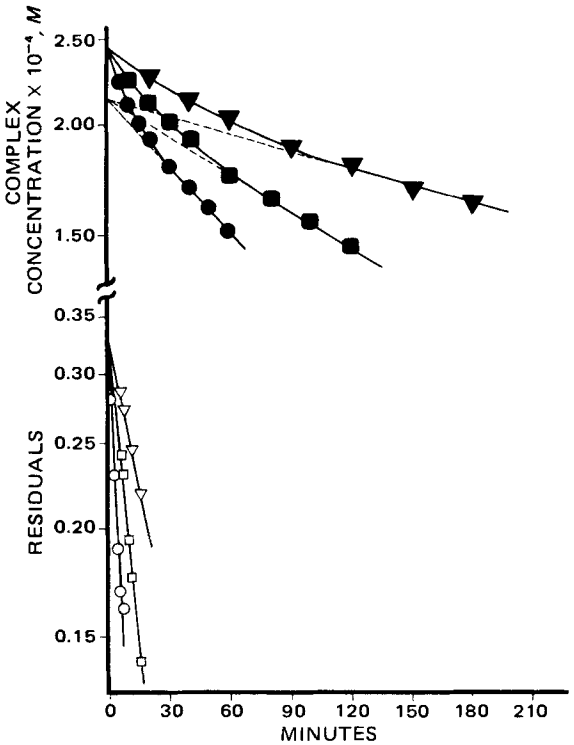

Figure 11—*Top: Semilogarithmic plot of complex concentration* $\times 10^{-4}$ M *undegraded* versus *time in minutes in acid halide catalysis experiment at pH 1.5 and 67° while varying the chloride-ion concentration. Key:* ▼, 1×10^{-2} M; ■, 3.3×10^{-2} M; *and* ●, 1×10^{-1} M. *Bottom: Semilogarithmic plot of residuals* $\times 10^{-4}$ M versus *time in minutes in acid halide catalysis experiment at pH 1.5 and 67° while varying the chloride-ion concentration and utilizing Eq. 10. Key:* ▽, 1×10^{-2} M; □, 3.3×10^{-2} M; *and* ○, 1×10^{-1} M.

applies as the solution to the data:

$$[Pd(X_2)L] = 0.237e^{-0.0653t} + 2.213e^{-0.00276t} \qquad \text{(Eq. 14)}$$

The proposed general reaction mechanism for acid halide catalysis is shown in Scheme V.

The coordination compound was reported to have antimitogenic and antiviral effects (20). Therefore, the chloride ligands are assumed to be displaceable while 2,6-diaminopyridine is a carrier ligand (5). The bidentate *cis*-complex must be employed, since the monodentate *cis*-complex can racemize into the thermodynamically more stable *trans*-configuration. Thus, the *cis*-configuration was postulated as necessary for activity (5), although it may not be stable.

A serious study of the stability of such complexes in the *cis*-configuration form is important for the understanding of their behavior in biological fluids. For example, the rate of chloride release and subsequent hydration of the complex molecule have been reported to be important steps in the mechanism of action. The chloride-ion concentration envi-

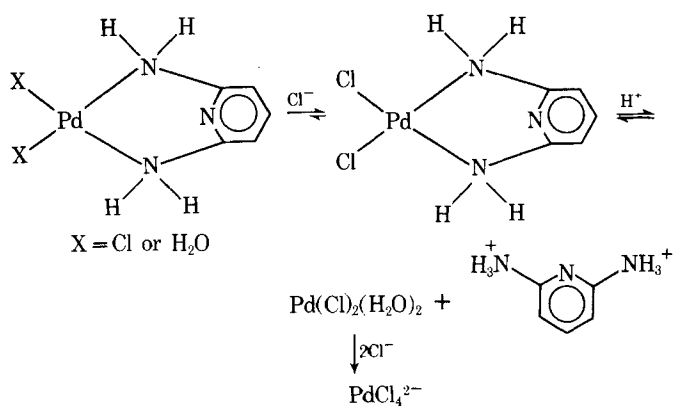

Scheme V

Table V—Calculated Values of A, B, α, and β Utilizing the Curve-Stripping Procedure for Acid Halide Catalysis

pH	Temperature	$[Cl^-]$, M	A, M	B, M	$\alpha \times 10^{-3}$, min^{-1}	$\beta \times 10^{-4}$, min^{-1}
1.10	37°	0.10	0.127	2.323	16.8	9.2
	37°	0.033	0.127	2.323	8.1	3.64
	47°	0.10	0.175	2.275	84.75	24.2
	47°	0.033	0.175	2.275	21.9	8.7
	47°	0.01	0.175	2.275	10.76	3.4
	57°	0.10	0.262	2.188	154.0	58.34
	57°	0.033	0.262	2.188	49.8	21.50
	57°	0.01	0.262	2.188	23.5	9.67
1.50	57°	0.10	0.237	2.213	65.3	27.6
	57°	0.033	0.237	2.213	27.9	13.0
	57°	0.01	0.237	2.213	16.6	5.76
	67°	0.10	0.322	2.128	130.0	50.7
	67°	0.033	0.322	2.128	60.7	31.7
	67°	0.01	0.322	2.128	23.7	14.7

ronment in the extra- and intracellular fluids can be a good justification for the alteration of anionic release and, therefore, activity.

REFERENCES

(1) B. Rosenberg, L. Van Camp, and T. Krigas, *Nature*, **205**, 698 (1965).

(2) B. Rosenberg, L. Van Camp, J. E. Trasko, and V. E. Mansour, *ibid.*, **222**, 385 (1969).

(3) J. A. Howle, G. R. Gale, and A. B. Smith, *Biochem. Pharmacol.*, **21**, 1465 (1972).

(4) A. B. Robins, *Chem.-Biol. Interact.*, **6**, 35 (1973).

(5) D. R. Williams, *Inorg. Chim. Acta Rev.*, **6**, 123 (1972).

(6) J. E. House, Jr., and M. J. Adams, *J. Inorg. Nucl. Chem.*, **32**, 345 (1970).

(7) R. Farrou and J. E. House, Jr., *ibid.*, **34**, 2219 (1972).

(8) L. I. Elding and L. Gustafson, *Inorg. Chim. Acta*, **5**, 643 (1971).

(9) L. I. Elding, *ibid.*, **6**, 647 (1972).

(10) *Ibid.*, **6**, 683 (1972).

(11) *Ibid.*, **7**, 581 (1973).

(12) D. Robb, N. M. De V. Steyn, and H. Kruger, *Inorg. Chim. Acta*, **3**, 383 (1969).

(13) A. J. Poe and D. H. Vaughan, *ibid.*, **1**, 255 (1967).

(14) R. G. Pearson and D. A. Johnson, *J. Am. Chem. Soc.*, **86**, 3983 (1964).

(15) J. S. Coe, J. R. Lyons, and M. D. Hussain, *J. Chem. Soc. A, Part I*, **1970**, 90.

(16) J. S. Coe, M. D. Hussain, and A. A. Malik, *Inorg. Chim. Acta*, **2**, 65 (1968).

(17) R. F. Coley and D. S. Martin, Jr., *ibid.*, **7**, 573 (1973).

(18) J. S. Coe and J. R. Lyons, *J. Chem. Soc. A, Part III*, **1969**, 2669.

(19) C. M. Davidson and R. F. Jameson, *Trans. Faraday Soc.*, **61**, 2462 (1965).

(20) H. A. Tayim, A. H. Malakian, and A. B. Bikhazi, *J. Pharm. Sci.*, **63**, 1469 (1974).

(21) C. E. Skinner and M. M. Jones, *J. Am. Chem. Soc.*, **91**, 1984 (1969).

ACKNOWLEDGMENTS AND ADDRESSES

Received November 24, 1975, from the *School of Pharmacy and the ‡Chemistry Department, American University of Beirut, Beirut, Lebanon.

Accepted for publication December 8, 1976.

Presented at the Basic Pharmaceutics Section, APhA Academy of Pharmaceutical Sciences, Atlanta meeting, November 1975.

Supported in part by a grant from the University Medical Research Fund, American University of Beirut.

ˣ To whom inquiries should be directed.

Microbiological Turbidimetric Methods: Linearization of Antibiotic and Vitamin Standard Curves

F. KAVANAGH

Abstract □ Procedures were devised to linearize the usually curved calibration lines for turbidimetric microbiological assays. Three new equations relating concentration of drug and turbidity are described; two are for antibiotic assays and one for vitamin assays. One equation is for antibiotic assays employing *Klebsiella pneumoniae* as the test organism. The accuracy of interpolation from the three equations was studied by means of appropriate mathematical models based on erythromycin, chlortetracycline (*K. pneumoniae*), and cyanocobalamin assays. The accuracy of the new expressions was significantly superior to those used previously, and they are of general applicability.

Keyphrases □ Microbiological turbidimetry—antibiotic and vitamin assays, procedures devised to linearize curved calibration lines □ Turbidimetry—microbiological antibiotic and vitamin assays, procedures devised to linearize curved calibration lines □ Antibiotics—microbiological turbidimetry assays, procedures devised to linearize curved calibration lines □ Vitamins—microbiological turbidimetry assays, procedures devised to linearize curved calibration lines

Nonlinear standard curves are much more common than straight lines in microbiological turbidimetric assays for growth-promoting substances and antibiotics. The nonlinear calibration line is particularly important in high accuracy assays because of the difficulty of obtaining sample potencies from it with negligible computational error. High accuracy assays are now possible not only from the automated system previously described (1) but also from manual assays. Therefore, the old practice of drawing a "best" straight line through the points of the standard line is no longer appropriate because the line, in reality, is curved. Approximating the slightly curved antibiotic lines by straight-line segments (2, 3) causes a small computational error.

Procedures for straightening both the antibiotic lines and the often more strongly curved vitamin lines are described in this report. Antibiotic lines will be considered separately from vitamin lines because they have different theoretical bases and the procedures have different principles.

Since an equation that truly fits a calibration line is not known, the line can only be approximated. The approximation can be fairly accurate when calibration points are close together. However, if the dose line can be linearized, fewer calibration points are needed to obtain the same accuracy of approximation. The aim of the present study